Biosensors and Bioelectronics 80 (2016) 208–214

Contents lists available at ScienceDirect

Biosensors and Bioelectronics

journal homepage: www.elsevier.com/locate/bios

Ultrasensitive electrochemical detection of nucleic acid by coupling an autonomous cascade target replication and enzyme/gold nanoparticle-based post-amplification

Shufeng Liu [a,*], Wenji Wei [a], Yanqun Wang [a], Li Fang [a], Li Wang [a,*], Feng Li [b,*]

[a] Key Laboratory of Sensor Analysis of Tumor Marker, Ministry of Education, College of Chemistry and Molecular Engineering, Qingdao University of Science and Technology, No.53, Rd. Zhengzhou, Qingdao, Shandong 266042, China
[b] College of Chemistry and Pharmaceutical Sciences, Qingdao Agricultural University, Qingdao, Shandong 266109, China

ARTICLE INFO

Article history:
Received 28 September 2015
Received in revised form
20 January 2016
Accepted 27 January 2016
Available online 28 January 2016

Keywords:
DNA biosensor
Electrochemistry
Target replication
signal amplification
Gold nanoparticle

ABSTRACT

Owing to the intrinsic importance of nucleic acid as bio-targets, the development of isothermal and ultrasensitive electrochemical DNA biosensor is very essential for biological studies and medical diagnostics. Herein, the autonomous cascade DNA replication strategy was effectively married with the enzyme/gold nanoparticle-based post-amplification strategy to promote the detection performance toward target DNA. A hairpin DNA probe (HP) is designed that consists of an overhang at 3′-end as the recognition unit for target DNA, a recognition site for nicking endonuclease, and an alkane spacer to terminate polymerization reaction. The autonomous DNA replication–scission–displacement reaction operated by the nicking endonuclease/KF polymerase induced the autocatalytic opening of HP, which was then specifically bound by the enzyme/gold nanoparticles for further dual-signal amplification toward target-related sensing events. A low detection limit of 0.065 fM with an excellent selectivity toward target DNA could be achieved. The proposed biosensor could be also easily regenerated for target detection. The developed biosensor creates an opportunity for the effective coupling of the target replication with post-amplification strategies and thus opens a promising avenue for the detection of nucleic acid with low abundance in bioanalysis and clinical biomedicine.

1. Introduction

The development of DNA biosensors capable of amplified detection of DNA is being greatly motivated by its potential applications in clinical and diagnostic research (Enkin et al., 2014; Turner, 2013; Zhao et al., 2014; Zhang et al., 2013; Liang et al., 2014; Lin et al., 2015; Sawyers, 2008; Hsieh et al., 2012). Up to date, different isothermal signal amplification strategies have been proposed for the fabrication of DNA biosensors (Wang et al., 2014a; Yan et al., 2014; Lei and Ju, 2012). The well-developed signal amplification strategy can be simply categorized as two distinct types: post-amplification strategy toward the signal produced by hybridization or recognition event, and target recycling strategy. Examples of post-amplification strategy includes the use of enzymes (Liu et al., 2008a; Patolsky et al., 2001; Wilner et al., 2009; Shen et al., 2015), metal nanoparticles (Zhang et al., 2006; Song et al., 2010; Shi et al., 2015), DNA concatamer (Liu et al., 2014; Chen et al., 2012; Russell et al., 2014), DNA bio-barcode (Zhang et al., 2009; Song et al., 2014) as amplifying labels. The target recycling strategy is usually operated via nucleases for example exonuclease, endonuclease, polymerase or DNAzyme, to devote for the indirect amplification toward target number (Gerasimova and Kolpashchikov, 2014; Zuo et al., 2010; Xuan et al., 2012a, 2012b; Kong et al., 2011; Xu et al., 2012; Lu et al., 2012). Although great advances have been made toward the target detection by using each of these two strategies, the development of biosensor with further upgraded detection performance is still highly desirable to satisfy the requirement for the profiling trace amounts of biomarkers, and then serve for the clinical early diagnosis and treatment of some major diseases. It is conceived that the effective combination of these two classes of strategies would be attractive to address this issue. Unfortunately, it has been rarely reported for the biosensor fabrication via the grafting or marriage of these two strategies (Kong et al., 2014; Liu et al., 2013a; Wang et al., 2013; Chen et al., 2013). Recently, the nicking endonuclease-based target recycling has been ingeniously associated with rolling circle amplification (RCA)-based post-amplification for the development of ultrasensitive DNA biosensor (Ji et al., 2012; Wang et al., 2014b). But the assay is relatively complex, and also the biosensor can not

* Corresponding authors.
E-mail addresses: sliu@qust.edu.cn (S. Liu), wangli@qust.edu.cn (L. Wang), lifeng@qust.edu.cn (F. Li).

http://dx.doi.org/10.1016/j.bios.2016.01.067
0956-5663/

be regenerated for the target DNA detection. The catalyzed hairpin DNA assembly (CHA)-based amplification strategy may be another choice for the coupling of target recycling and post-amplification (Yin et al., 2007; Qing et al., 2014; Jung and Ellington, 2014; Li et al., 2012). But the CHA strategy is usually restricted with the relatively rigor design principle for the adopted hairpin DNA. Recently, the development of DNA machine has attracted substantial concerns owing to its striking improvement for the detection performance toward target analytes (Wang et al., 2012; Lu et al., 2013; Yao et al., 2015; Duan et al., 2013; Weizmann et al., 2008). The most typical example is based on the autonomous replication–scission–displacement strategy by means of nicking endonuclease and polymerase (Yin et al., 2013; Zhuang et al., 2014; Freage et al., 2014; Weizmann et al., 2006; Wang et al., 2012; Chen et al., 2015). Accompanied with the DNA replication–scission–displacement process, the target analogs could be exponentially produced for the remarkable signal amplification. It thus holds a great promise to substitute PCR due to its easy operation, isothermal reaction, and high sensitivity. However, this autonomous DNA replication strategy is more preferentially connected with the fluorescence technique. By comparison, electrochemical method can provide significant advantages, such as its inherent signal stability, low cost, high sensitivity and ease of calibration (Xuan et al., 2012a, 2012b; Ren et al., 2014; Ronkainen et al., 2010; Rowe et al., 2011; Hu et al., 2014). Also, the instrumentation can be easily integrated with some miniaturized devices or lab-on-a-chip platforms. Considering the remarkable signal amplification capability of this machine-like DNA replication–scission–displacement strategy, it is therefore convinced that the effective coupling with the appropriate electrochemical signal readout or reporter system would offer a promising avenue for the ultrasensitive electrochemical detection of DNA.

Herein, the autonomous cascade DNA replication strategy was effectively married with the enzyme/gold nanoparticle-based post-amplification strategy for the first time to fabricate an ultrasensitive electrochemical DNA biosensor. A hairpin DNA probe (HP) is designed that consists of an overhang at 3′-end as the recognition unit for target DNA, a recognition site for nicking endonuclease, and an alkane spacer to terminate polymerization reaction. The assay protocol for target DNA mainly involves the following two modules: (1) autonomous DNA replication–scission–displacement module operated by the nicking endonuclease/KF polymerase for the indirect amplification toward target amounts and autocatalytic opening of HP to expose the caged DNA fragment in the stem region of the 5′-end of HP; (2) enzyme/gold nanoparticle-based dual-signal amplification module toward the above target-related sensing events. Also, this isothermal signal amplification reaction operated by the nicking endonuclease/KF polymerase involves no damage or cleavage toward the original probe DNA, indicating that it may be beneficial for the fabrication of the regenerated and amplified electrochemical DNA biosensor. The current proposed strategy creates an effective grafting for the target replication and post-amplification strategies and thus holds a huge potential for the detection of nucleic acid with low abundance in bioanalysis and clinical biomedicine.

2. Experimental section

2.1. Materials and chemicals

Tris(2-carboxyethyl)phosphine (TCEP), 6-Mercapto hexanol (MCH) and 1-Naphthyl phosphate (1-NP) were purchased from Sigma-Aldrich (St. Louis, MO, USA). Nb.BbvCI endonuclease, Klenow Fragment (3′→5′ exo-) (KF polymerase), and deoxyribonucleoside triphosphates (dNTPs) were purchased from New England Biolabs, Inc. (Beverly, MA, USA). Bovine serum albumin (BSA) and streptavidin-alkaline phosphatase (SA-ALP) were obtained from Beijing Dingguo Biotechnology Company (Beijing, China). Fetal bovine serum was purchased from Sangon Biotech Co., Ltd. (Shanghai, China). All of the other chemicals were of analytical reagent grade and used without further purification. The HPLC-purified oligonucleotide sequences are purchased from Sangon Biotech. Co., Ltd. (Shanghai, China) and listed in Table S1.

2.2. Apparatus.

All electrochemical measurements were carried out by using a CHI 660D electrochemical workstation (CH Instruments, Shanghai, China) at room temperature. A conventional three-electrode system was used, which comprised a gold working electrode (2 mm diameter), a platinum wire auxiliary electrode, and a Ag/AgCl reference electrode. TEM images were obtained using an FEI Tecnai (G2 20 TWIN) TEM at an acceleration voltage of 200 KV (FEI Company, USA). The particle size were measured using dynamic light scattering technique on a Malvern Zetasizer 3000 HS (Malvern Instruments, Worcestershire, UK).

2.3. Electrode pretreatment.

The gold electrode was cleaned by immersion in a freshly prepared piranha solution (a 3:1 v/v mixture of concentrated H_2SO_4 and 30% H_2O_2) for 20 min, followed by a thorough rinsing with ultrapure water. Then the electrode was polished on a microcloth (Shanghai Chenhua Inc., China) with 50 nm alumina slurry to obtain a mirror surface, followed by sonication in acetone and ultrapure water for 5 min each, to remove residual alumina powder. The well-polished electrode was then subjected to electrochemical pretreatment by cycling the potential between −0.2 and 1.5 V in H_2SO_4 (0.5 M) at a scan rate of 100 mV s^{-1} until a stable cyclic voltammogram was obtained, and then the cleaned electrode was allowed to be dried at room temperature.

2.4. Preparation of signal probe (SP) DNA conjugated gold nanoparticle (SP-AuNP).

The gold nanoparticles (AuNPs) with diameter of about 13 nm were prepared as reported previously (Grabar et al., 1995). Simply, after heating 100 mL of 1 mM $HAuCl_4$ solution to 100 °C, 10 mL of 38.8 mM trisodium citrate was added quickly to the boiling solution under continuous stirring. The reaction mixture was stirred at 100 °C for 15 min until the color turned red and then stored at 4 °C. A volume of 50 μL biotin-labeled signal probe DNA (SP1 DNA) (10 μM) was then added to 1 mL of AuNPs solution and stirred at room temperature overnight. Afterward, 0.1 mL of PBS containing 2 M NaCl was added to the mixture stepwise for stabilizing the obtained AuNPs probe, which was centrifuged at 10,000 rpm and washed with PBS twice, and then resuspensed in 0.5 mL of PBS (Qian et al., 2014). The SP1 DNA conjugated AuNPs (SP1-AuNPs) were characterized by UV–vis spectra (Fig. S1 in the Supporting Information). The characteristic absorption peak of AuNPs was red-shifted from 521 to 525 nm due to the decoration of SP1 DNA on AuNPs (Wang et al., 2014c). It could be also seen from Fig. S2 that the average hydrodynamic size for SP1-AuNPs was evidently increased than that of the bare AuNPs. The increased size came from the conjugated SP1 DNA on the AuNPs (Wang et al., 2015; Zheng et al., 2013). Furthermore, the obtained AuNPs and SP1-AuNPs were also characterized by TEM techniques (Fig. S3). No evident change about the size and morphology for each SP1-AuNP could be observed compared with that of the bare AuNP.

2.5. The immobilization of hairpin DNA (HP) on the electrode surface

Each DNA solution was heated to 95 °C for 5 min and then allowed to cool to room temperature before use. The above-treated gold electrode was incubated into 10 mM Tris–HCl (10 mM TCEP, 0.5 M NaCl, pH 7.4) containing 0.5 μM HP DNA for 12 h at room temperature. The HP immobilized electrode was subsequently immersed in 0.5 mM MCH solution for 1 h to remove the non-specific DNA adsorption.

2.6. Autonomous cascade DNA replication and hybridization with SP1-AuNPs

The above HP immobilized electrode was then incubated into 50 μL 20 mM Tris–HCl buffer (140 mM NaCl, 5 mM $MgCl_2$, pH 7.4) containing 8 U of Nb.BbvCI endonuclease, 6 U of Klenow fragment exo-, 0.8 mM dNTPs and different concentrations of target DNA for 2 h at 37 °C. Then, the electrodes were taken out and rinsed with 10 mM Tris–HCl buffer (0.5 M NaCl, pH 7.4). The above electrode was then incubated into 50 μL SP1-AuNPs solution for 2 h and rinsed with 10 mM Tris–HCl buffer (0.5 M NaCl, pH 7.4). A BSA solution (20 μL of 2% BSA) was dropped onto the electrode and incubated at 37 °C for 30 min to block the nonspecific site. Then, 20 μL 5 μg/ml SA-ALP solution was added onto the electrode surface and incubated at 37 °C for 40 min.

2.7. Electrochemical detection

The Differential pulse voltammetric (DPV) results were recorded in 100 mM Tris–HCl buffer (1 mM $MgCl_2$, pH 9.0) containing 4 mM 1-NP with the potential window from 0 V to 0.6 V, the pulse amplitude of 50 mV and the pulse period of 0.2 S. The electrochemical impedance spectra (EIS) were recorded in 1 mM $[Fe(CN)_6]^{3-/4-}$ and 0.1 M KNO_3 with the frequency range from 0.1 Hz to 10 kHz. Before measurements, the electrolyte solution should be thoroughly purged with high purity nitrogen for about 20 min.

2.8. Regeneration of the DNA biosensor

The regeneration of the DNA biosensor was operated by first de-hybridization in hot water (95 °C) for 15 min. Then the de-hybridized electrode was transferred into 70 μL 10 mM Tris–HCl (pH 7.4, 0.5 M NaCl) and heated to 95 °C for 5 min, and then allowed to cool to 37 °C for 1 h.

3. Results and discussion

3.1. Design of strategy

In this work, the autonomous cascade target replication strategy was effectively grafted with the enzyme/gold nanoparticle-based signal amplification for the achievement of ultrasensitive detection of nucleic acid. The fabrication principle of the biosensor was schematically demonstrated in Scheme 1. A hairpin-like probe DNA (HP) is designed, which could be divided into three main domains labeled with I, II and III. The domain I at the 3′-end of HP is used for the recognition unit for the target DNA. The base sequences at the 5′-end of HP (domain III) is caged in the stem region by the complementary base sequences in the domain II. An 18-carbon spacer is inserted between domain II and III to terminate the polymerization reaction. The base sequences located between domains I and II could be used as the Nb.BbvCI endonuclease recognition related site. When the target DNA is present, it hybridizes with the domain I of the HP and then triggers the polymerization reaction driven by the added KF polymerase. The polymerization reaction yields a new replicate across the HP template part including Nb.BbvCI recognition related site and domain II. Herein, the introduced alkane spacer can accurately

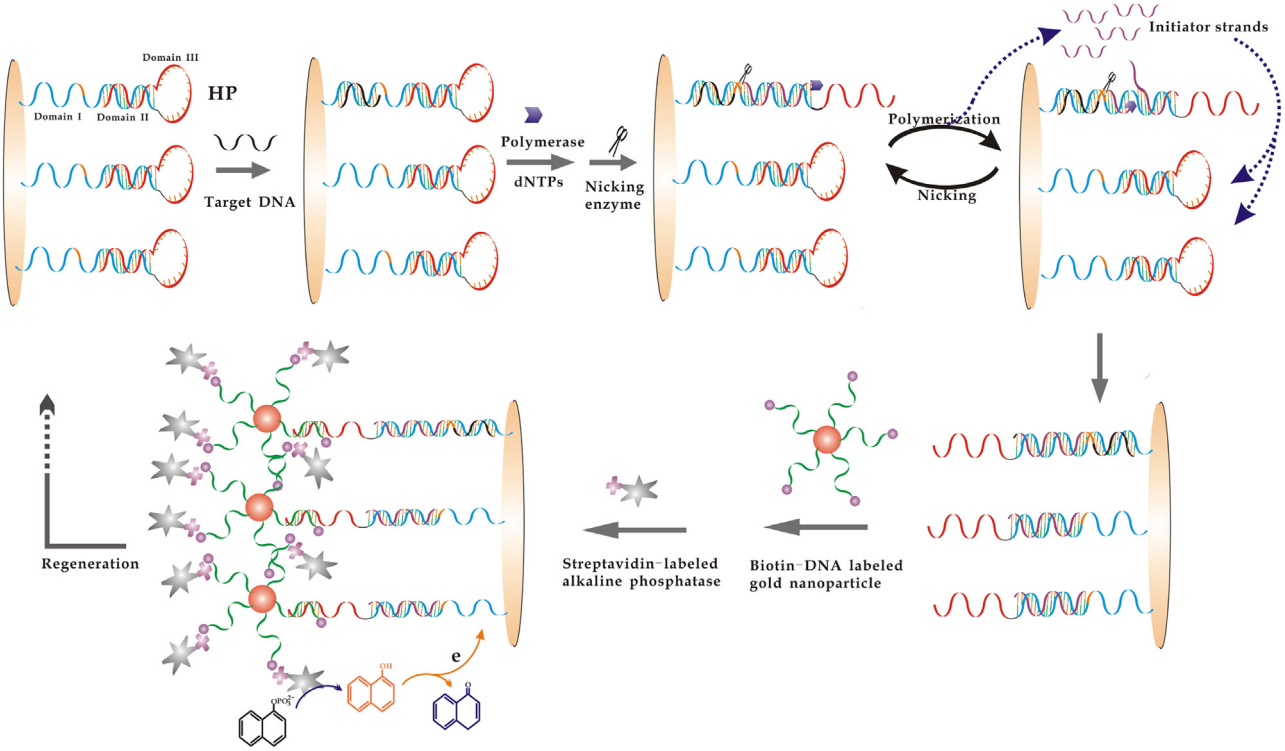

Scheme 1. The schematic illustration for target DNA detection by the coupled autonomous cascade target replication and enzyme/gold nanoparticle-based post-amplification strategy.

terminate polymerization reaction at the end of domain II. Meanwhile, the domain III would be displaced from the duplex structure of stem. Moreover, along with the formation of the recognition sites for Nb. BbvCI nicking endonuclease between domain I and domain II, an autonomous cleavage–replication–displacement reaction process operated by nicking endonuclease and KF polymerase is then underwent, simultaneously generated a large amount of ssDNA fragment (Van Ness et al., 2003; Jia et al., 2010; Wang et al., 2013). These produced new ssDNA fragment could be used as the secondary target for the direct hybridization with the domain II of the HP to open more new HPs and expose the domain III. The liberated domain III of the HP is then hybridized with the signal probe DNA (SP1 DNA) linked onto the gold nanoparticle (SP1-AuNP) for further signal amplification. It should be noted that the SP1-AuNP is very difficult to directly hybridize with the HP owing to the caging effect of the complementary base sequences at the 5′-end of HP (domain III). The SP1-AuNP is used as the signal amplification carrier owing to the binding of a large amount of SP1 for each AuNP. The 5′-end of the SP1 was labeled with a biotin group. Thus, once the HP is opened and the domain III is exposed, the SP1-AuNP could be linked onto the electrode surface. The streptavidin-alkaline phosphatase (SA-ALP) could be linked onto the electrode surface by the specific affinity reaction with biotin. The ALP then catalyzes conversion of electrochemically inactive 1-naphthyl phosphate (1-NP) into an electrochemically active phenol for the generation of a remarkable electrochemical response. Therefore, the whole biosensing strategy for nucleic acid could be divided into two separate modules: autonomous cascade target replication module for the indirect amplification toward target amounts; enzyme/gold nanoparticle-based dual-signal amplification module toward the target-related biosensing events.

3.2. *Feasibility of the fabricated DNA biosensor for target DNA detection.*

The feasibility of the proposed electrochemical biosensor for target DNA detection was firstly verified by DPV method (Fig. 1A). A distinct electrochemical oxidation signal at the potential of about 0.28 V was obtained in the coexistence of target DNA, nicking endonuclease and KF polymerase (curve d in Fig. 1A). However, only a very weak electrochemical response could be obtained in the case of no target DNA (curve a in Fig. 1A), which could be simply attributed to the non-specific adsorption of SA-ALP onto the electrode surface. Almost the same background response could be only obtained for the control experiment conducted in the presence of target DNA but no polymerase (curve b in Fig. 1A), indicating that the HP could be hardly opened to expose the domain III for the further binding of AuNPs and SA-ALP. Furthermore, it could be also found that the electrochemical response in the absence of nicking endonuclease was evidently lower than that in the coexistence of nicking endonuclease and KF polymerase (curve c in Fig. 1A). The above control experiments in the absence of nicking endonuclease or KF polymerase strongly verified that the signal amplification capability of the autonomous cleavage–replication–displacement process for target DNA detection. The electrode modification and biosensor fabrication was also confirmed by electrochemical impedance spectroscopy (EIS) measurements (Fig. 1B). The EIS data were fitted by an equivalent electrical circuit (inset, Fig. 1B). An almost straight line was observed with the charge transfer resistance (Rct) value of 310 Ω for the bare gold electrode (curve a in Fig. 1B), which was typical characteristics of a mass diffusion-controlled electrode transfer process. Nevertheless, after the assembly of the HP and MCH on the electrode, a big semicircle with Rct value of about 4065 Ω could be observed (curve b in Fig. 1B), indicating an evident increase of the charge transfer resistance, which could be ascribed to the repellence of $Fe(CN)_6^{3-/4-}$ from approaching electrode surface by negative-charged phosphate skeletons of HP DNA. After the target-induced autonomous cleavage–replication–displacement process toward HP by nicking endonuclease/KF polymerase, a decreased Rct value of about 3383 Ω was observed (curve c in Fig. 1B), which might be considered based on the following factors. The formed rigid dsDNA increased the negative charge on the electrode surface, which might hinder the electrode transfer. However, the opened HP might promote the accessibility of Fe $(CN)_6^{3-/4-}$ toward electrode surface compared with the caged HP with the densely packed structure, which increased the electrode transfer ability (Yang et al., 2012; Liu et al., 2013b). Herein, the latter might dominate for the observed decreased Rct value. Furthermore, after the binding of SP1-AuNPs on the electrode surface, the diameter of the semicircle increased evidently with the Rct value of about 5173 Ω (curve d in Fig. 1B). Although the AuNPs have often been verified to improve electron transfer ability of the redox species, herein the introduction of more amounts of SP1 DNA on the AuNPs surface increased the negative charge of the electrode surface for the decreased interfacial charge transfer. Furthermore, the affinity reaction for the binding of SA-ALP on the electrode surface evidently increased the charge transfer resistance with the Rct value of about 7921 Ω (curve e in Fig. 1B).

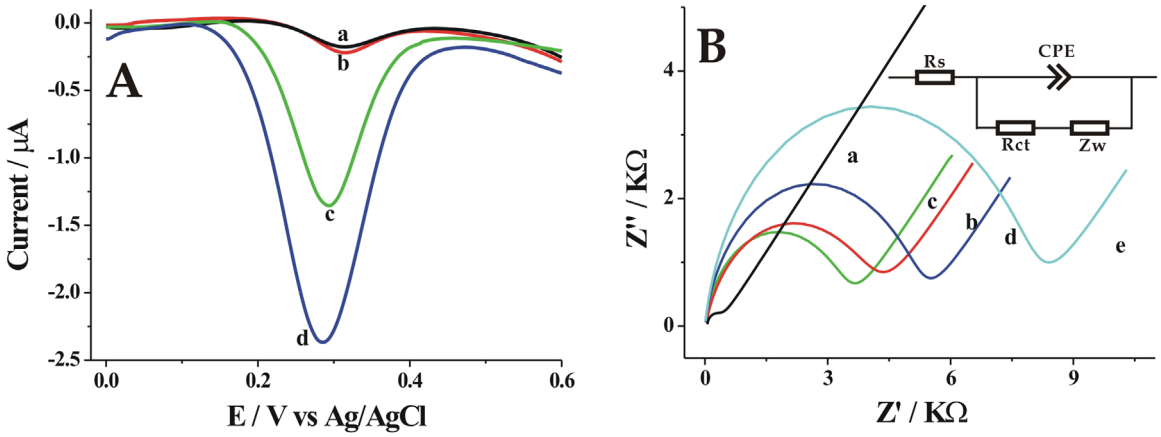

Fig. 1. (A) DPV of the fabricated electrochemical DNA biosensor. The curves a and d are the corresponding DPV responses in the absence and presence of 10 pM target DNA, respectively. The curves of b and c are for the control experiments conducted in the absence of KF polymerase or nicking endonuclease, respectively. (B) EIS of the different modified electrodes. The curves were obtained for bare gold electrode (a), the HP and MCH modified electrode (b), the recognition toward 10 pM target DNA in the presence of nicking endonuclease and KF polymerase (c), the further binding with SP-AuNPs (d), and the affinity interaction with SA-ALP (e), respectively.

This could be easily understood that the bulky protein molecule binding on the electrode surface largely inhibit the approaching of $Fe(CN)_6^{3-/4-}$ toward electrode surface. The EIS experiments could further provide beneficial supports for the biosensor fabrication process by the coupled autonomous cascade target replication and enzyme/gold nanoparticle-based signal amplification strategy.

In order to further verify the contribution of the binding of SA-ALP by the affinity interaction on the electrode surface for the ultimate electrochemical response toward target DNA, we also use SP2 as a substitute of SP1 for the labeling on the AuNPs. The SP2 is not labeled by a biotin group at the 5′-end. It indicated that no SA-ALP could be easily linked onto the electrode surface. It could be seen from Fig. S4A that the ultimate electrochemical response toward target DNA detection was only slightly larger than the background response in the absence of target DNA. This fully indicated that electrochemical response was indeed originated from the specifically linked SA-ALP. Also, in order to further evidence that the inserted 18-carbon spacer between domain II and III contributes the termination of polymerization reaction for the exposed domain III and then for the linking of SP1-AuNPs on the electrode surface, we also designed a HP2 that contained no such spacer. It could be seen from Fig. S4B that almost the same background signal could be only obtained. We also used a biotin-labeled signal probe DNA (SP3) to directly hybridize with the opened HP DNA after the autonomous cascade target replication process for target DNA detection, which was compared with that by using SP1-AuNPs. It could be seen from Fig. S5 that the SP1-AuNPs could exert an evidently larger electrochemical response than that by using SP3 only. This also evidenced the signal amplification effect of the AuNPs for target DNA detection.

3.3. The optimization of experimental conditions

The surface density of SP1 DNA on the AuNPs may have an important effect on the detection performance toward target DNA. It was simply controlled by using three different concentrations of SP1 DNA during the preparation of SP1-AuNPs (Liu et al., 2008b). It could be seen from Fig. S6 that the employed SP1 DNA concentration of 10 μM during the preparation of SP1-AuNPs could achieve the better electrochemical response than that at other two concentrations. The higher concentration of SP1 DNA would increase the surface density of SP1 DNA on the AuNPs, which may restrict the recognition efficiency of the SP1-AuNPs to the opened HP owing to the steric hindrance effect. In order to further achieve the best sensing performance, the corresponding experimental conditions including the amounts of Nb.BbvCI nicking endonuclease, KF polymerase and the reaction time were also optimized (Fig. S7). The optimized amounts of the Nb.BbvCI nicking endonuclease and KF polymerase were chosen as 8.0 and 6.0 Units, respectively (Fig. S7A and B). The time dependence of the autonomous cascade target replication process operated by nicking endonuclease and KF polymerase for target response were shown in Fig. S7C. The optimized time for the autonomous cascade target replication process was determined as 2 h.

3.4. Detection sensitivity of the developed DNA biosensor

To further confirm the ability of the proposed biosensor to sensitively detect target DNA, a series of different concentrations of target DNA ranging from 0 to 10 pM were measured (Fig. 2A). The electrochemical intensity was observed to increase with the concentration of target DNA, indicating that the autonomous cascade target replication process on the electrode surface was highly dependent on the concentration of target DNA. A good linear relationship between the DPV peak current and the logarithm value of the target DNA concentration ranging from 0.1 fM to 1 pM could be obtained (Fig. 2B). The regression equation was $Y=0.42\ \lg X+7.09$ (Y and X represented the DPV peak current and target DNA concentration, respectively; unit of X was M) with the correlation coefficient of 0.9965. The detection limit, which was defined as 3 times the standard deviation of the background, was about 0.065 fM. This detection limit is superior or comparable with that of the mostly reported electrochemical DNA biosensors (Table S2).

In order to further verify the capability of the coupled autonomous cascade target replication and enzyme/gold nanoparticle-based signal amplification strategy for target DNA detection, we also conducted the target DNA detection in the absence of nicking endonuclease. It indicated that no autonomous cleavage–replication–displacement process could be realized, but the target DNA-induced polymerization reaction could be still able to open the HP for the binding of enzyme/gold nanoparticle. It could be seen from Fig. 3 that the electrochemical intensity increased also with target DNA concentration (Fig. 3A). A good linear relationship between the DPV peak current and the logarithm value of the target DNA concentration ranging from 0.1 pM to 1 nM could be also obtained (Fig. 3B). The regression equation could be listed as $Y=0.52\ \lg X+7.10$ with the correlation coefficient of 0.9957. A low detection limit of about 0.056 pM toward target DNA could be only obtained, which was about three order of magnitudes higher than

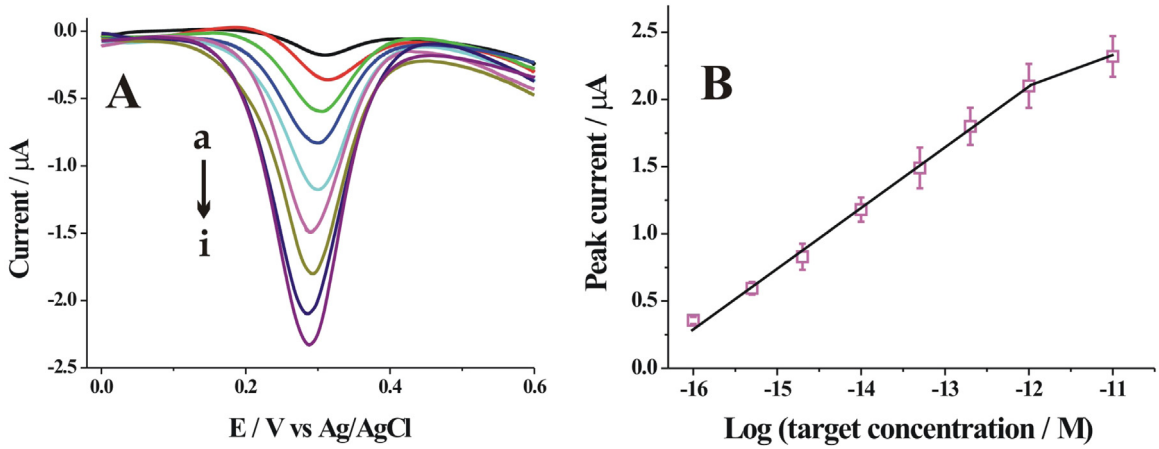

Fig. 2. (A) DPV responses corresponding to the analysis of different concentrations of target DNA. The concentrations of target DNA for the curves (a) to (i) are: (a) 0, (b) 0.1 fM, (c) 0.5 fM, (d) 2 fM, (e) 10 fM, (f) 50 fM, (g) 200 fM, (h) 1 pM, and (i) 10 pM. (B) The linear relationship between the DPV peak current and the logarithm value of the target DNA concentration. Error bars represent standard deviations of measurements ($n=3$).

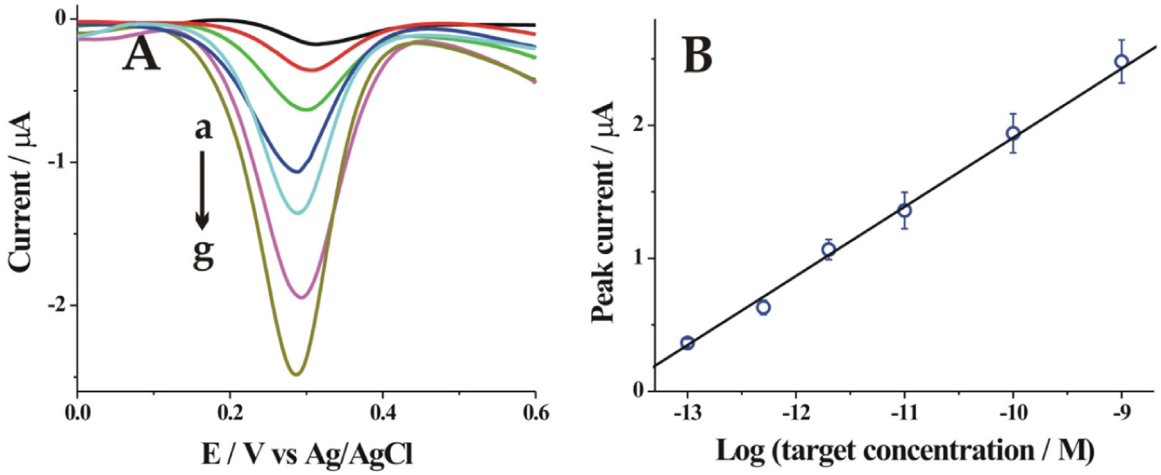

Fig. 3. (A) DPV responses corresponding to the analysis of target DNA in the absence of nicking endonuclease. The concentrations of target DNA for the curves (a) to (g) are: (a) 0, (b) 0.1 pM, (c) 0.5 pM, (d) 2 pM, (e) 10 pM, (f) 100 pM, and (g) 1 nM; (B) The linear relationship between the DPV peak current and the logarithm value of the target DNA concentration. Error bars represent standard deviations of measurements ($n=3$).

that of the coupled autonomous cascade target replication and enzyme/gold nanoparticle-based post-amplification strategy.

3.5. Selectivity, stability and regeneration of the developed DNA biosensor

The specificity of the developed DNA biosensor was further investigated by using three kinds of DNA sequences, including complementary target DNA (TD), single-base mismatched DNA (1MT), two-base mismatched DNA (2MT) and non-complementary DNA (NC) (Fig. 4). The DPV peak current responses toward 1MT and 2MT were about 34.4% and 16.2% of that for perfect target DNA at the same concentration, respectively, indicating a good performance to discriminate perfect complementary target and the mismatched targets. We also conducted the target DNA detection in a relatively complex biological matrix (5% fetal bovine serum). Comparable responses could be obtained for the detection of three different concentrations of target DNA in both buffer and diluted serum (Fig. S8), indicating the potential of the fabricated electrochemical biosensor for the detection of target DNA in the relatively complex biological sample.

The stability for the HP modified electrode has also been checked. Three independent experiments demonstrated that the HP DNA modified electrode could retain about 94.1% of its initial response toward target DNA after its storage in the refrigerator at 4 °C for a week, indicating a relatively robust stability of the modified electrode (Fig. S9). Furthermore, the fabricated DNA biosensor could be regenerated for the successive detection toward target DNA. It could be seen from Fig. 5 that the effective detection toward target DNA could be still realized even after its regeneration for three times. Also, the regenerated electrode could still demonstrate the background signal in the absence of target DNA (data no shown). It should be noted that some nuclease-based target recycling or replication strategies for signal amplification are very difficult to execute the regeneration experiments owing to the specific cleavage or some other treatment toward the immobilized parent probe DNA on the electrode surface.

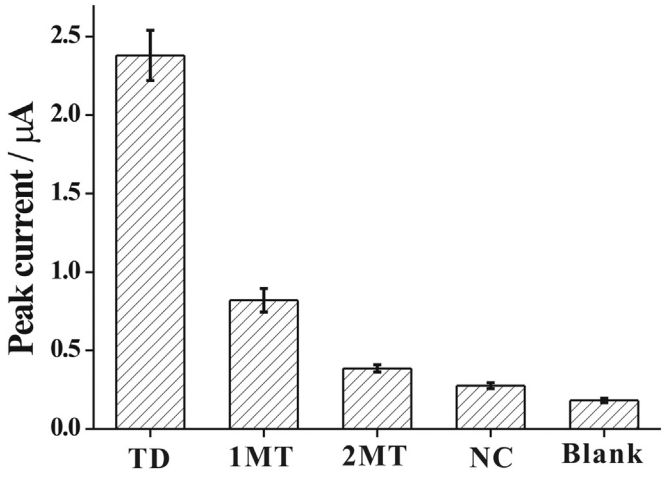

Fig. 4. The bar chart of the DPV responses toward blank and different DNA sequences including TD, 1MT, 2MT and NC at the same concentration of 10 pM.

4. Conclusion

In conclusion, an isothermal and ultrasensitive electrochemical DNA biosensor was fully developed by the effective coupling of the autonomous cascade DNA replication and enzyme/gold nanoparticle-based post-amplification strategies. The autonomous DNA

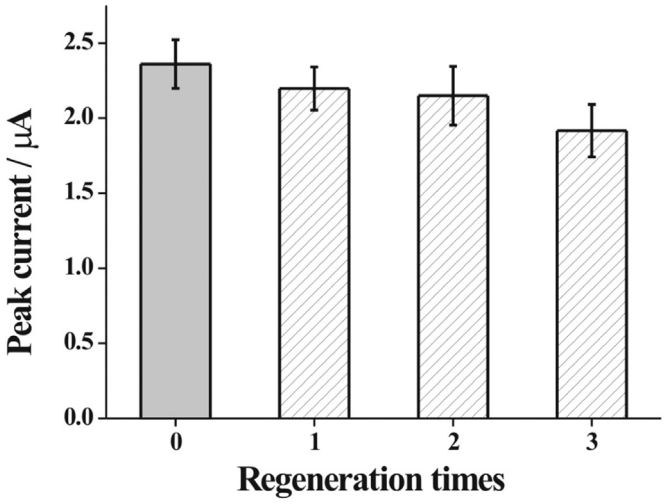

Fig. 5. The regeneration experiments of the propose DNA biosensor for the target DNA detection. The Bar 0 represents the original electrochemical responses toward 10 pM target DNA. The Bars 1, 2 and 3 represents the electrochemical responses of the regenerated HP1 modified electrode. The number indicates the regeneration times.

replication–scission–displacement reaction operated by the nicking endonuclease/KF polymerase endows the indirect and autocatalytic amplification toward target amounts. The enzyme/gold nanoparticle affords the successive dual-signal post-amplification toward target-related sensing events. A low detection limit of 0.065 fM with an excellent selectivity toward target DNA could be achieved. The proposed biosensor could be also easily regenerated for target detection. It thus opens a promising avenue for the fabrication of ultrasensitive and regenerated electrochemical DNA biosensor and holds a huge potential in bioanalysis and clinical diagnostics.

Acknowledgment

This work was funded by the National Natural Science Foundation of China (Nos. 21475072 and 21575074), the Natural Science Foundation of Shandong Province of China (Nos. ZR2015JL007, ZR2014BM019), the Basic Research Program of Qingdao (No. 13-1-4-214-jch) and the Special Foundation for Taishan Scholar of Shandong Province.

Appendix A. Supplementary material

Supplementary data associated with this article can be found in the online version at http://dx.doi.org/10.1016/j.bios.2016.01.067.

References

Chen, A., Gui, G., Zhuo, Y., Chai, Y., Xiang, Y., Yuan, R., 2015. Anal. Chem. 87, 6328–6334.
Chen, X., Hong, C.Y., Lin, Y.H., Chen, J.H., Chen, G.N., Yang, H.H., 2012. Anal. Chem. 84, 8277–8283.
Chen, Y., Wang, Q., Xu, J., Xiang, Y., Yuan, R., Chai, Y., 2013. Chem. Commun. 49, 2052–2054.
Duan, R., Zuo, X., Wang, S., Quan, X., Chen, D., Chen, Z., Jiang, L., Fan, C., Xia, F., 2013. J. Am. Chem. Soc. 135, 4604–4607.
Enkin, N., Wang, F., Sharon, E., Albada, H.B., Willner, I., 2014. ACS Nano 8, 11666–11673.
Freage, L., Wang, F., Orbach, R., Willner, I., 2014. Anal. Chem. 86, 11326–11333.
Gerasimova, Y.V., Kolpashchikov, D.M., 2014. Chem. Soc. Rev. 43, 6405–6438.
Grabar, C.K., Freeman, R.G., Hommer, M.B., Natan, M.J., 1995. Anal. Chem. 67, 735–743.
Hsieh, K., Patterson, A.S., Ferguson, B.S., Plaxco, K.W., Soh, H.T., 2012. Angew. Chem. Int. 51, 4896–4900.
Hu, J., Yu, Y., Brooks, J.C., Godwin, L.A., Somasundaram, S., Torabinejad, F., Kim, J., Shannon, C., Easley, C.J., 2014. J. Am. Chem. Soc. 136, 8467–8474.
Ji, H., Yan, F., Lei, J., Ju, H., 2012. Anal. Chem. 84, 7166–7171.
Jia, H., Li, Z., Liu, C., Cheng, Y., 2010. Angew. Chem. Int. 49, 5498–5501.
Jung, C., Ellington, A.D., 2014. Acc. Chem. Res. 47, 1825–1835.
Kong, R.M., Zhang, X.B., Zhang, L.L., Huang, Y., Lu, D.Q., Tan, W., Shen, G.L., Yu, R.Q., 2011. Anal. Chem. 83, 14–17.
Kong, R.M., Song, Z.L., Meng, H.M., Zhang, X.B., Shen, G.L., Yu, R.Q., 2014. Biosens. Bioelectron. 54, 442–447.
Lei, J., Ju, H., 2012. Chem. Soc. Rev. 41, 2122–2134.
Liang, H., Zhang, X.B., Lv, Y., Gong, L., Wang, R., Zhu, X., Yang, R., Tan, W., 2014. Acc. Chem. Res. 47, 1891–1901.
Li, B., Jiang, Y., Chen, X., Ellington, A.D., 2012. J. Am. Chem. Soc. 134, 13918–13921.
Lin, M., Wang, J., Zhou, G., Wang, J., Wu, N., Lu, J., Gao, J., Shi, J., Zuo, X., Fan, C., 2015. Angew. Chem. Int. 54, 2151–2155.
Liu, C.W., Huang, C.C., Chang, H.T., 2008a. Langmuir 24, 8346–8350.
Liu, G., Wan, Y., Gau, V., Zhang, J., Wang, L., Song, S., Fan, C., 2008b. J. Am. Chem. Soc. 130, 6820–6825.
Liu, S., Lin, Y., Liu, T., Cheng, C., Wei, W., Wang, L., Li, F., 2014. Biosens. Bioelectron. 56, 12–18.
Liu, S., Wang, C., Zhang, C., Wang, Y., Tang, B., 2013b. Anal. Chem. 85, 2282–2288.
Liu, S., Wang, Y., Ming, J., Lin, Y., Cheng, C., Li, F., 2013a. Biosens. Bioelectron. 49, 472–477.
Lu, C.H., Wang, F., Willner, I., 2012. J. Am. Chem. Soc. 134, 10651–10658.
Lu, C.H., Willner, B., Willner, I., 2013. ACS Nano 7, 8320–8332.
Patolsky, F., Lichtenstein, A., Willner, I., 2001. Nat. Biotechnol. 19, 253–257.
Qian, R., Ding, L., Yan, L., Lin, M., Ju, H., 2014. Anal. Chem. 86, 8642–8648.
Qing, Z., He, X., Huang, J., Wang, K., Zou, Z., Qing, T., Mao, Z., Shi, H., He, D., 2014. Anal. Chem. 86, 4934–4939.
Ren, K., Wu, J., Zhang, Y., Yan, F., Ju, H., 2014. Anal. Chem. 86, 7494–7499.
Ronkainen, N.J., Halsall, H.B., Heineman, W.R., 2010. Chem. Soc. Rev. 39, 1747–1763.
Rowe, A.A., Chuh, K.N., Lubin, A.A., Miller, E.A., Cook, B., Hollis, D., Plaxco, K.W., 2011. Anal. Chem. 83, 9462–9466.
Russell, C., Welch, K., Jarvius, J., Cai, Y., Brucas, R., Nikolajeff, F., Svedlindh, P., Nilsson, M., 2014. ACS Nano 8, 1147–1153.
Sawyers, C.L., 2008. Nature 452, 548–552.
Shen, Q., Han, L., Fan, G., Zhang, J.R., Jiang, L., Zhu, J.J., 2015. Anal. Chem. 87, 4949–4956.
Song, S., Qin, Y., He, Y., Huang, Q., Fan, C., Chen, H.Y., 2010. Chem. Soc. Rev. 39, 4234–4243.
Song, W., Li, H., Liang, H., Qiang, W., Xu, D., 2014. Anal. Chem. 86, 2775–2783.
Shi, M., Zheng, J., Tan, Y., Tan, J., Li, J., Li, Y., Li, X., Zhou, Z., Yang, R., 2015. Anal. Chem. 87, 2734–2740.
Turner, A.P.F., 2013. Chem. Soc. Rev. 42, 3184–3196.
Van Ness, J., Van Ness, L.K., Galas, D.J., 2003. Proc. Nat. Acad. Sci. USA 100, 4504–4509.
Wang, C., Zhou, H., Zhu, W., Li, H., Jiang, J., Shen, G., Yu, R., 2013. Biosens. Bioelectron. 47, 324–328.
Wang, F., Elbaz, J., Willner, I., 2012. J. Am. Chem. Soc. 134, 5504–5507.
Wang, F., Lu, C.H., Willner, I., 2014a. Chem. Rev. 114, 2881–2941.
Wang, Q., Yang, C., Xiang, Y., Yuan, R., Chai, Y., 2014b. Biosens. Bioelectron. 55, 266–271.
Wang, W.J., Li, J.J., Rui, K., Gai, P.P., Zhang, J.R., Zhu, J.J., 2015. Anal. Chem. 87, 3019–3026.
Wang, X.P., Yin, B.C., Wang, P., Ye, B.C., 2013. Biosens. Bioelectron. 42, 131–135.
Wang, Z., Sun, N., He, Y., Liu, Y., Li, J., 2014c. Anal. Chem. 86, 6153–6159.
Weizmann, Y., Cheglakov, Z., Willner, I., 2008. J. Am. Chem. Soc. 130, 17224–17225.
Weizmann, Y., Beissenhirtz, M.K., Cheglakov, Z., Nowarski, R., Kotler, M., Willner, I., 2006. Angew. Chem. Int. Ed. 45, 7384–7388.
Wilner, O.I., Weizmann, Y., Gill, R., Lioubashevski, O., Freeman, R., Willner, I., 2009. Nat. Biotechnol. 4, 249–254.
Xu, H., Wang, L., Ye, H., Yu, L., Zhu, X., Lin, Z., Wu, G., Li, X., Liu, X., Chen, G., 2012. Chem. Commun. 48, 6390–6392.
Xuan, F., Luo, X., Hsing, I.M., 2012a. Anal. Chem. 84, 5216–5220.
Xuan, F., Luo, X., Hsing, I.M., 2012b. Biosens. Bioelectron. 35, 230–234.
Yao, G.H., Liang, R.P., Yu, X.D., Huang, C.F., Zhang, L., Qiu, J.D., 2015. Anal. Chem. 87, 929–936.
Yan, L., Zhou, J., Zheng, Y., Gamson, A.S., Roembke, B.T., Nakayama, S., Sintim, H.O., 2014. Mol. BioSyst. 10, 970–1003.
Yang, N., Cao, Y., Han, P., Zhu, X., Sun, L., Li, G., 2012. Anal. Chem. 84, 2492–2497.
Yin, B.C., Liu, Y.Q., Ye, B.C., 2013. Anal. Chem. 85, 11487–11493.
Yin, P., Choi, H.M.T., Calvert, C.R., Pierce, N.A., 2007. Nature 451, 318–322.
Zhang, H., Li, F., Dever, B., Li, X.F., Le, X.C., 2013. Chem. Rev. 113, 2812–2841.
Zhang, J., Song, S., Zhang, L., Wang, L., Wu, H., Pan, D., Fan, C., 2006. J. Am. Chem. Soc. 128, 8575–8580.
Zhang, X., Su, H., Bi, S., Li, S., Zhang, S., 2009. Biosens. Bioelectron. 24, 2730–2734.
Zhao, W.W., Xu, J.J., Chen, H.Y., 2014. Chem. Rev. 114, 7421–7441.
Zheng, J., Zhu, G., Li, Y., Li, C., You, M., Chen, T., Song, E., Yang, R., Tan, W., 2013. ACS Nano 7, 6545–6554.
Zhuang, G., Tang, D., Lai, W., Chen, G., Yang, H., 2014. Anal. Chem. 86, 8400–8407.
Zuo, X., Xia, F., Xiao, Y., Plaxco, K.W., 2010. J. Am. Chem. Soc. 132, 1816–1818.